Journal of Physics Communications

PAPER

On a rapidly converging iterative algorithm for diode parameter extraction from a single *IV* curve

Enrico Cataldo[1], **Alberto Di Lieto**[1,2], **Francesco Maccarrone**[1] and **Giampiero Paffuti**[1,2]

[1] University of Pisa, Physics Department, Largo Pontecorvo 3, Pisa, IT, Italy
[2] INFN, Largo Pontecorvo 3, Pisa, IT, Italy

E-mail: enrico.cataldo@unipi.it

Keywords: semiconductor diodes, current–voltage characteristic, semiconductor device model, nonlinear iterative fitting

OPEN ACCESS

RECEIVED
8 June 2017

REVISED
11 October 2017

ACCEPTED FOR PUBLICATION
25 October 2017

PUBLISHED
13 December 2017

Abstract

We measure the *I–V* curve of a *p–n* diode on a range of currents where the well known Shockley model exhibits its shortcoming. We show that the behavior of the *I–V* curve, on the whole range of currents, can be captured by a modified four parameter Shockley model; the parameters of the model are obtained by a numerical procedure, consisting of an iterative rapidly converging nonlinear fitting algorithm. The fit returns sound estimates of the parameters for *I–V* curves, as function of temperature. The method is validated on a well known 1N4148 diode, but it can also be applied to any other devices described by single-diode models such as solar cells. We also show that the knowledge of the temperature dependence of the parameters can be used to obtain a quantitative estimate of other physical properties of the system, such as the energy gap of junction materials.

1. Introduction

Current–voltage (*I–V*) curves are routinely used to give synthetic graphical information of the behavior of non-ohmic electronic components such as semiconductor diodes [1] or other rectifying devices as Schottky diodes both in the most common metal-semiconductor realization [2] or in the recent graphene-semiconductor structure [3]. The modeling of such components through an equivalent electrical circuit is necessary to include a device in a numerical simulator such as those of the SPICE type. In several circumstances accurate values of the model parameters are not given by the manufacturers or they are dependent on the environmental parameters, e.g. the temperature. Therefore a practical procedure to evaluate the relevant parameters from a single measure of the current crossing the diode as a function of the applied external voltage V is desirable and it is widely discussed by many authors [4–7]. In general, the extraction of the parameters of a given model from the measured *IV* curves is a non-trivial task, since the *I–V* dependence is usually expressed in an implicit form. Numerical fitting procedures are often involved and require a previous graphical inspection of the experimental curves. In the following we shall treat the case of a *pn* junction diode which minimal model requires four parameters. As the single-diode parametrization is currently used also in the assessment of the performances of photovoltaic systems [4, 7, 8], the choice of the semiconductor diode is justified with the aim of demonstrating the validity of the method by the possibility of a comparison with the available technical data.

In fact, the ideal *I–V* characteristic of a *p–n* junction is, at the basic level, approximated by the popular Shockley equation [1]:

$$I = I_S\left[\exp\left(\frac{V}{nV_T}\right) - 1\right]. \tag{1}$$

The properly called Shockley equation has the *non-ideality factor n* equal to unity, and it is appropriate only for ideal junctions. For real junctions, n is greater than 1. The *thermal voltage* $V_T = kT/e$ has a value of 25.8 mV at room temperature.

The saturation current I_S describes the level of conductivity of the diode, and ideally it coincides with the value of the current when a large reverse voltage is applied to the junction. It depends (in a very complex way) on

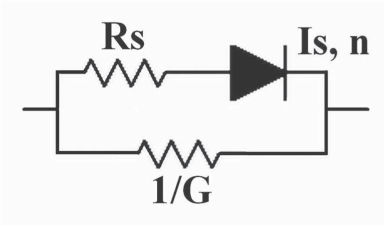

Figure 1. Electrical circuit corresponding to the four parameters model of the real diode.

the constructive parameters of the diode, such as the area and the depth of the junction, or the doping spatial uniformity. It is possible to express its main dependence on the temperature following the argument that I_S grows with the population of the conducting level of the semiconductor carriers in accordance with a stationary thermodynamic distribution:

$$I_S = I_A \exp\left(-\frac{E_G}{nkT}\right), \tag{2}$$

where E_G is the energy gap of the bulk semiconductor and the dependence of I_A from T is here neglected.

It is worth to note that, using an argument similar to that explaining the non-ideality factor n in the Shockley equation, the same factor must be taken into account in the exponential dependence of I_S. However, the presence of n in (2) is sometimes omitted. Although in the real diodes the value of n is only approximately constant with V, in a quite large interval of direct currents (1) reproduce well the I–V curve with constant values of I_S and n, and these two parameters can be easily determined with elementary fitting procedure, even graphical. In fact, when $V \gg nV_T$, the logarithmic graph of the current show a clear linear trend. The dependence of the fitted value of n on the portion of the characteristic curve examined has already been discussed previously [9]. On the other hand, significant deviation from the behavior predicted by the model of equation (1) are observed on both sides, of large and very low currents. In the first case, direct current is lower than that predicted by the model, and the exponential trend is weakened so that the logarithmic graph stays under the straight line calculated at intermediate current. On the contrary, at lower current, a larger direct current is observed.

The origin of the large current deviation can be explained as the lowering of the voltage difference across the junction with respect to the applied *fem* because of ohmic voltage drop in the semiconductor bulk hosting the junction. On the other hand, the low current regime originates from the presence of alternative paths for the current. When the junction current is very low, these parallel paths give a comparable contribution to the total current. The different dependence on V can be only observed when the exponential term is not the dominant source.

Then, a more accurate model for the DC I–V characteristic of the diode can be formulated by introducing a series resistance R_s, accounting for the ohmic voltage drop across the semiconductor bulk, and a parallel resistance $1/G$, accounting for alternative paths [10–13]: figure 1 shows the equivalent electrical circuit; this model has four parameters, and equation (1) modifies into:

$$I = I_p + I_J = GV + I_S[\exp B(V - R_s I_J) - 1], \tag{3}$$

Where I_J is the current flowing into the junction, $I_p = GV$ is the current flowing into the parallel resistance and $B = e/nkT$; a similar model is analyzed in [14].

It is worth mentioning again that I–V characteristic measurements are used for the assessment of the performances of conventional photovoltaic cells and single-diode models of these devices are largely applied to several photovoltaic devices [8], which attracted a growing interest in the last few years. Parallel and series resistances are normally introduced in the modelization of the photovoltaic cell and in the evaluation of its performance [15], so that the method illustrated for the semiconductor diode should be also valuable for these devices. A good discussion of the state of the art of the applied numerical methods in that field is found in a recent paper [16].

To increase the quality of the fit of experimental data, some authors [17] proposed junction models consisting of a sum of exponentials, sometimes called two-diode or multiple diode models, each with multiple I_S and n parameters. Each contribution is considered valid in different regions of the I–V curve and some kind of connection in the contiguous regions is required. The weakness of these strategies is the lack of an underlying simple physical picture and the increase of the number of model parameters.

In this paper we describe an experiment using an apparatus, directed into a LabVIEW environment, for the recording of IV curves of a semiconductor diode at different temperatures in a large range of currents (from 10 nA to 10 mA). A simple and reliable procedure to extract the model parameters from the measurements in the

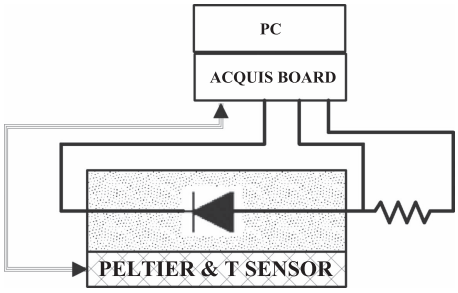

Figure 2. Schematic view of the experimental setup.

full range of currents explored is presented and the comparison with Shockley equation and with a three parameters model including only the series resistance is discussed. The results are compared with the parameter reported in the current literature and the validity of the method is also proved by the study of the dependence of the saturation current on the temperature, showing that the data extracted gives a value of the barrier height of the junction in accordance with the current knowledge.

2. Experimental

2.1. Apparatus

A small ($3 \times 3 \times 2$ cm^3) brass cube is placed between two 30 W thermoelectric power sources/sinks assembled with commercial Peltier modules (see figure 2). It hosts both the device being tested, a commercial 1N4148 silicon *p–n* diode, and a calibrated thermistor. The system stabilizes the temperature of the central volume of the cube in a few tens of seconds to the value set by the operator in the range 10 °C–100 °C with an accuracy better than 1 °C. The *I–V* characteristic is then measured with two differential channels of a National Instruments NI6221 data acquisition board equipped with multiplexed 16 bit ADC with selectable bipolar full scales. One of the ADC channels samples the voltage V across the electrodes of the diode with a resolution of 0.3 mV and the other channel senses the current I crossing the diode by measuring the potential drop on a calibrated resistor R in series with the diode, with a nominal resolution of 0.02 μA, given by the combination of 10 nA (absolute) and 5×10^{-5} (relative). V is varied applying to the series diode-R the variable signal of a digital-to-analog channel (DAC) of the NI6221 board. The control of the thermal cycle and of the data taking is programmed devising a LabVIEW virtual instrument. Initially, a set of temperatures is selected by the operator. After this, the controlled thermal cycles operate until the value of each T is stable into a few tenths of °C. The couples (V, I) are saved in a file and are labeled with the temperature measured just before and just after the voltage scan. The difference of two readings of the temperature is ever less than 0.5 °C in absolute value, the sign being dependent on the direction of the last heat flux cycle. Thereby, we can evaluate that the value of the diode temperature is known with an average precision of 0.2 °C.

2.2. Results and discussion

Figure 3 shows the plot of $\log(I)$ versus V for the full range of applied voltages. The measured currents spans more than six order of magnitude ranging from few nA to 10 mA. The zone of linearity of the experimental *I–V* characteristic in the logarithmic scale indicates, at a glance, the region where an exponential dependence of I on V is likely. In the linear region, $\exp(B) \gg 1$, so equation (1) ca be simplified to:

$$I = A \exp(BV). \tag{4}$$

Limiting the analysis to this region a nonlinear fit of the last equation, through a standard least square routine[3], gives a value of $B = e/nkT = 19.48 \pm 0.03$ V^{-1}, largely different from the ideal diode constant at the same temperature $B_{\mathrm{id}} = e/kT = 36.20$ V^{-1}. The agreement of the model with the data requires a value:

$$n = \frac{B_{\mathrm{id}}}{B} = 1.86 \pm 0.01$$

which is lower than the value of the SPICE models for 1N4148 diode. The SPICE model published by NXP Semiconductors reports a value $n = 1.906$ (see http://nxp.com/documents/spice_model/1N4148.prm), but agrees with other experiments [18], pointing out the variability of this parameter due to constructive tolerance or details of data analysis. The curve superimposed to the experimental data in (figure 3) is the best fit obtained with

[3] Consider for reference the functions `lsqnonlin` of the `MatLab` libraries or `leasqrdemo` of the `Octave` packages.

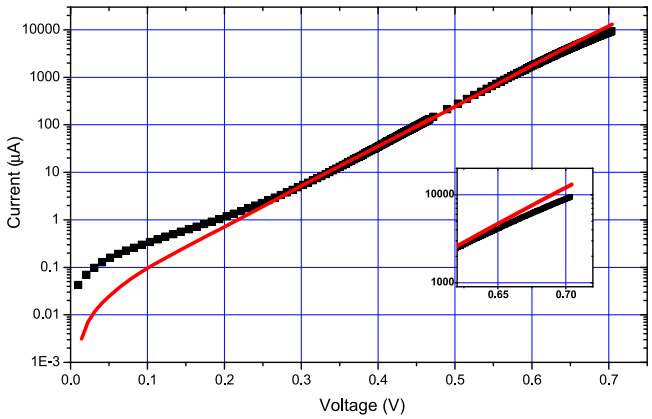

Figure 3. *I–V* data at $T = 47.8$ °C plotted in semi-logarithmic scale. The continuous line is the best fit curve obtained with the Shockley model (1)with two parameters applied to the data with $2\ \mu\text{A} < I < 120\ \mu\text{A}$. The inset is a zoom of the high current data. It is evident that at very low currents ($I < 1\ \mu$A) and at high current ($I > 1$ mA) the *minimal* model is not accurate.

equation (4), applied to data of the region of moderate currents. It is evident that the two-parameter model systematically underestimates lower values of the current and overestimates its higher values. A more realistic comprehension of the nature of the different contributions to the diode current, therefore, requires a study of these limiting regimes.

As explained in the Introduction, besides the two parameters of the Shockley equation I_S and n, two supplementary parameters must be taken into account: the parallel conductance G and the series resistance R_s and the full model is given by equation (3). At very low values of the current the correction due to the series resistance is negligible and the model simplifies into:

$$I = GV + I_S(\exp BV - 1) \tag{5}$$

with I and V being the current and the voltage sensed at the diode leads, as before.

Some authors [14] declare the unsuitability of the analysis of the forward *I–V* curve to find G and suggest the extraction of this parameter through a graphical treatment of the reverse biased diode characteristic. Indeed, for $V \ll nV_T$ the linear approximation of the exponential brings a linear relation between the current and the voltage:

$$I = (G + BI_S)\,V \tag{6}$$

which is not useful to calculate G unless I_S and B are known or if the second term of the function of equation (6) is negligible, as in this case ($BI_S \simeq 0.2\ \mu$S). As a matter of fact, we find it suitable to apply the same least square nonlinear fitting routine using equation (5) as the model equation. As the first term GV gives an appreciable contribution only at very low values of V we limit the experimental data up to a guess threshold current I_0. The value of the small signal conductance G can be determined executing the corresponding numerical fit with three parameters, I_s, B and G.

The result of the fitting procedure are shown graphically in figure 4 and the found values for parameters are reported in the caption. It is worth noting that I_S and B values are not in accordance with those extracted with the minimal model in the central range of the currents. This confirms that the calculated ideality factor n depends on which part of the *I–V* curve is used in its evaluation.

At the higher values of the diode current, the series resistance R_s becomes important, while the small admittance G gives a negligible contribution. We may then rewrite equation (3) [10] as:

$$V(I) = \frac{1}{B}\log\left(\frac{I}{I_S} + 1\right) + R_s I \tag{7}$$

which can be used as a fit model for the *I–V* data at higher currents, giving the best values of the three parameters I_S, B and R_s. The result is shown in figure 5, and the found values for parameters are reported in the caption.

The values of the parameter B are approximately coincident, by few percent, in the two parts of the curve and the coincidence is maintained by varying the value of I_0. The values of the saturation currents differ by the order of ten percent, and the agreement is better for higher temperatures. The value of R_s is comparable with other measurements found in literature, although there is a wide spread of reported values (e.g. [19]). We were not able to find a reliable value of G for the 1N4148 diode in the literature.

In conclusion, the two sets of parameters obtained by fitting data with model equation (5) for the region $I < I_0$ and with model equation (7) for the region $I > I_0$, where I_0 is of the order of tens of μA, show some

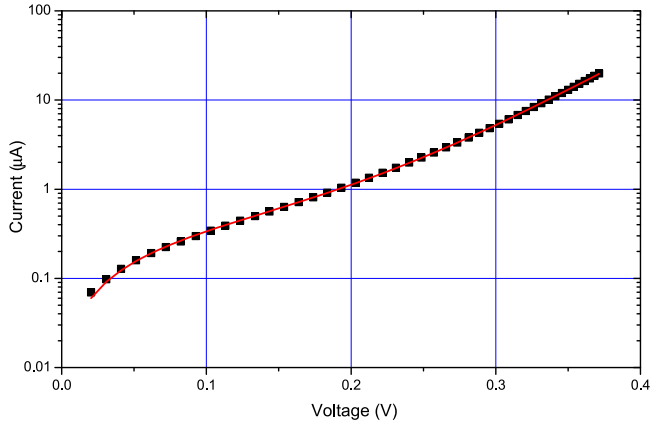

Figure 4. *I–V* data corresponding to the temperature $T = 47.8$ °C limited to $I < I_0 = 20$ μA. The continuous line is the result of the fit of experimental data (black square) with the model of equation (5). The fitted parameters are $Is = 9.72 \pm 0.17$ nA, $B = q/nkT = 20.30 \pm 0.05$ V^{-1} and $G = 2.75 \pm 0.01$ μS.

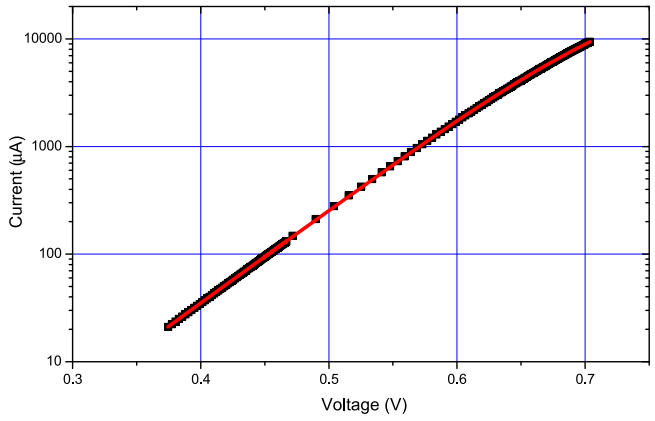

Figure 5. *I–V* data corresponding to the temperature $T = 47.8$ °C selected with $I > I_0 = 20$ μA. The continuous line is the result of the fit of experimental data (black square) with the model of equation (7). The fitted parameters are $Is = 13.4 \pm 0.12$ nA, $B = 19.78 \pm 0.02$ V^{-1} and $R_s = 2.32 \pm 0.03$ Ω.

discrepancies and a better analysis for the complete range of current is needed and it is presented in the following section.

3. Data analysis

The analysis presented in the previous paragraph clearly shows that the first term of equation (3) is significant only in the very low current region (see figure 4), while at higher currents the exponential term dominates and the second term alone is able to describe the experimental data well (see figure 5). This physical argument is the starting point of a numerical procedure which allows us to consider all the data together, using an iterative calculation. In general, a four parameter search in a nonlinear fitting procedure is a hard mathematical problem. The procedure can be highly unstable. In our specific case, in order to overcome this issue and to ensure the convergence of the algorithm, we have envisaged a method, which, by means of an appropriate first choice, notably reduce the complexity of the problem and makes it solvable. We start the iteration in region of low currents, where the parameter space collapses, effectively but not formally, from four to one dimension. This allows to find a first reliable value for one parameter. After that, the iterative procedure is applied, which is, as well known, one of the fastest method in numerical calculus. We verified, for all of the measurements performed, the convergence of the parameters toward stable and physically meaningful values, always in no more than 5 iterations, for the precision required.

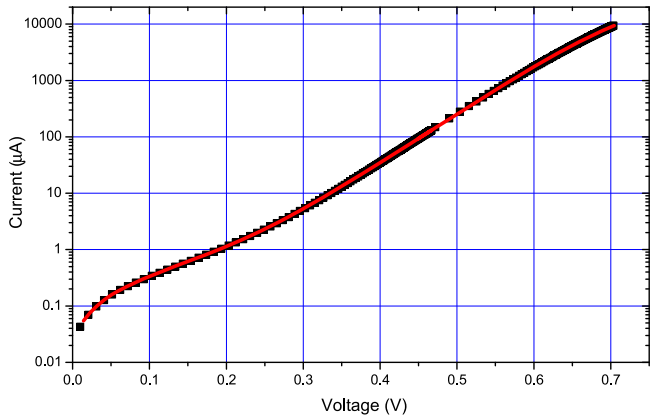

Figure 6. *I–V* data corresponding to the temperature $T = 47.8$ °C. The line is the result of the iterative fitting procedure described in the text. The agreement is good in the full range of the currents considered with $I_S = 10.5 \pm 0.2$ nA , $B = 20.2 \pm 0.1$ V^{-1}, $R_s = 2.75 \pm 0.05\ \Omega$ and $G = 2.80 \pm 0.05\ \mu Si$.

3.1. Single fitting procedure

By substituting $I_J = I - GV$ in the argument of the exponential of equation (3), an equation $I = f(I,\ V)$ could be written as the objective function of a fitting procedure suitable for models expressed in an implicit form. Nevertheless, this kind of algorithms is very complex and frequently suffers from numerical instabilities.

Here we describe an alternative method, based on an iterative fitting procedure for models expressed in an explicit form, leading to the simultaneous determination of four parameters necessary to reproduce the DC diode characteristic in a large region of currents. This method can be summarized in a few steps, including the iteration described in the loop section, where i is the flowing index, I, I^i and I_J^i are respectively the experimental values, computed values and computed junction values of the current:

(1) The first few data at very low currents are used to compute a first guess $G^i\,(i=0)$ of the parallel conductance with a linear fit of the model $I = GV$.

(2) *Begin loop* $I_J^i = I - G^iV$ gives the estimate of the junction current.

(3) The explicit model $V = V(I_J)$ of equation (7) is fitted with the data calculated at step 2 and the estimate of I_s^i, B^i and R_s^i is found.

(4) Updated values of the junction current I_J^{i+1} are found solving numerically equation (7) with the measured V and assuming the estimate of the three parameters I_S^i, B^i and R_s^i.

(5) Updated values of total current I^{i+1} are computed as $I^{i+1} = G^iV + I_J^{i+1}$.

(6) The first few data of I^{i+1} are compared to I to obtain the new value G^{i+1}: $I - I^{i+1} = \delta GV$, $G^{i+1} = G^i + \delta G$.

(7) *End loop* The four parameters with index $i + 1$ are compared to previous values: if the change is much less than the estimate of their errors the loop ends, otherwise it continues, returning to step 2.

It is worthwhile to note that the solutions of equation (7) (see step 4 of the algorithm above) are Lambert functions, whose values are known. We preferred to use a self-consistent and general approach, which can be easily adapted to different junction models.

Our method and the one using the Lambert function agree very well. After a few iterations the four parameters converge toward stable values and the procedure may be stopped. The final result is shown in the figure 6 where the agreement of the model with the experimental data is very good over the entire range. Table 1 shows the extracted parameters with the different models presented, using data of a specific current region when needed. The last set is obtained by using the iterative fitting procedure.

3.2. Determination of energy band gap from temperature dependence of parameters

In this section we extract energy band gap from the temperature dependence of I_S parameter, fitting *I–V* data taken at temperature between 10 and 100 °C. E_G is not explicitly present in the Shockley equation as it is enclosed only in the saturation current I_S; a more detailed expression of equation (2) is given by:

Table 1. Experimental parameters of the models for the *I–V* data at $T = 47.8$ °C

	G (μS)	R_s (Ω)	I_S (nA)	B (V^{-1})	n
Minimal model	—	—	14.63 (0.16)	19.48 (0.03)	1.856
Low I (equation (5))	2.75 (0.01)	—	9.72 (0.17)	20.30 (0.05)	1.783
High I (equation (7))	—	2.32 (0.03)	13.4 (0.12)	19.78 (0.02)	1.830
Full curve (equation (3))	2.80 (0.05)	2.75 (0.05)	10.5 (0.2)	20.2 (0.1)	1.790

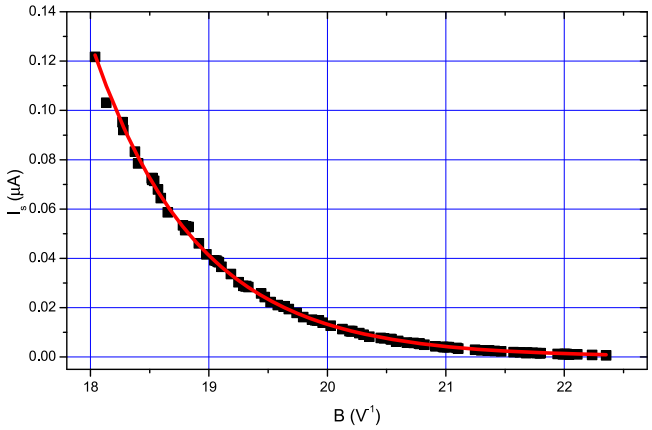

Figure 7. I_S as a function of B for 100 *I–V* curves analyzed with the iterative fitting procedure, described in the past subsection. The continuous curve represents the exponential *fit* with the simplified dependence $I_S = I_A e^{-BE_G}$. The agreement is rather good and the best value of the parameters are $I_A = 68 \pm 2$ *A* and $E_G = 1.117 \pm 0.002$ eV. The latter is in very close agreement with the tabulated value of the gap energy in Silicon at a temperature around 300 K.

$$I_S = AT^2 \exp\left(-\frac{E_G}{nkT}\right), \tag{8}$$

where A depends on the geometry of the junction and on the doping densities in the device.

There are two counteracting effects of an increase of n on the diode current. An increase of n causes a decrease of the current I in equation (1) the other parameters being fixed but, on the other hand, the same increase determines an increase of I_S, at a given temperature. Because of the larger value of E_G with respect to the voltage across the junction, the effect on I_S prevails and at fixed parameters, an increase of n entails an increase of I.

The need to consider the factor $1/n$ in the exponential in equation (8) can be justified by our data, by tracing the graph of I_S as a function of temperature, as determined by the exponential fit. The result is shown in figure 7 where a large set of curves *I–V*, taken in a two hour period, are analyzed. The weak power dependence on T can be neglected with respect to the exponential and the fit of the data is performed with the simplified model:

$$I_S = I_A \exp(-BE_G)$$

keeping the B parameter defined above in the place of e/nkT and expressing E_G in eV. With this position the resulting parameters are $I_A = 68 \pm 2$ *A* and $E_G = 1.117 \pm 0.002$ eV.

Other experiments using different data processing methods on Si *p–n* junction assert a close agreement with the accepted *band-gap* value of 1.12 eV at 300 K. For example, [20] report a value of 1.13 ± 0.02 eV, operating with the base-emitter junction of a Si bipolar transistor (2N3645 model), in the temperature interval $(-75, 25)$ °C. It is not easy to find fabrication details of the 1N4148 diode and particularly information on the doping levels. Based exclusively on [21], the 1N4148 is fabricated by growing a slightly doped ($<10^{16}$ cm^{-3}) *n-type* Si micro-metric layer onto an heavily doped substrate n^+ at dopant concentration of 10^{19} cm^{-3}. On the other side of *n*-layer an acceptor dopant is then diffused forming a *p* layer with doping density of 10^{19} cm^{-3}. With these levels of dopant a *band-gap narrowing* of several tens of meV is predicted and observed [22] and could conveniently be taken into account to adjust the expected value of E_G.

Our determination of E_G is based on an approximate model but conceivably the T^δ factor in the $I_S(T)$ relation should be considered. It is easy to understand that as this factor increases with temperature, the simplified model underestimates diode current at higher temperatures and the characteristic constants of the exponential in function of T lowers with respect to the value calculated without the power-like factor. We perform a nonlinear fit with the model:

$$I_S(T) = AT^{\delta} e^{-BE_G}.$$

We take $\delta = 1.5$, which is the common choice for many different diodes, and the best fit gives the value of 1.040 ± 0.005 eV for E_G. The best fit A value results $A = 2.5 \pm 0.2$ mA/K$^{1.5}$. The two parameters are strongly correlated so that an overestimation of the exponential characteristic constant involves an underestimation of the factor A and the E_G value is 80 meV lower than the one expected and with the disposable literature data [23–25]. This could be explained in terms of a high doping level at 2 to 3 $\times$ 10^{19} cm^{-3}.

4. Conclusion

We use the direct current–voltage characteristic data of a silicon diode 1N4148 to validate an iterative nonlinear fitting algorithm for parameter extraction of diode models of increasing complexity. The entire procedure of measurement and modeling can be easily automated integrating the data collection performed in a LabVIEW environment with suitable numerical packages. The four parameters of the modified Shockley model, represented in equation (7), are extracted and their values are found in quite good agreement with the literature. The advantages of the method presented here rely on the possibility to extract model parameters from data collected on a single large span of I values, and to easily compare simpler models.

It is worth noting that in the literature is reported that to extract the four parameters, by means of only the direct I–V characteristic, is difficult and cumbersome. This is an active area of research, in which periodically the state of the art is summarized in review articles such as [6] for the Schottky diode, [8] for the solar cells and [5] for the diode and solar cells, just to cite a few of them. Moreover, the method of I–V characteristic is also used in different research areas, such as, for example, [26]. As can be seen by reading these papers, the methods are several and in general the number of fitting parameters can be higher than four and moreover the relatioship between the parameters and the underlying physical processes can be difficult to establish. Our approach allows to obtain globally the four parameters in a straightforward manner and represents a possible solution of the above cited difficulties.

A confirmation of the validity of the analysis is given through the evaluation of the junction barrier E_G which results within a few percent in accordance with the accepted one.

ORCID iDs

Enrico Cataldo https://orcid.org/0000-0001-8589-9323
Alberto Di Lieto https://orcid.org/0000-0002-4787-0754
Francesco Maccarrone https://orcid.org/0000-0003-3710-9694
Giampiero Paffuti https://orcid.org/0000-0002-5145-4358

References

[1] Neudeck G W 1989 *The PN Junction Diode* 2nd edn (Reading, MA: Addison-Wesley)
[2] Sharma B L (ed) 1984 *Metal-Semiconductor Schottky Barrier Junctions and Their Applications* (Springer US)
[3] Chen C C, Aykol M, Chang CC, Levi AFJ and Cronin SB 2011 Graphene-silicon Schottky diodes *Nano Lett.* **11** 1863
[4] Cotfas D T, Cotfas P A and Kaplanis S 2013 Methods to determine the dc parameters of solar cells: a critical review *Renew. Sustain. Energy Rev.* **28** 588
[5] Ortiz-Conde A, García-Sánchez F J, Muci J and Sucre-González A 2014 A review of diode and solar cell equivalent circuit model lumped parameter extraction procedures *Facta Univ. Ser.: Electron. Energ.* **27** 57
[6] Olikh O Y 2015 Review and test of methods for determination of the Schottky diode parameters *J. App. Phys.* **118** 024502
[7] Jordehi A R 2016 Parameter estimation of solar photovoltaic (PV) cells: a review *Renew. Sustain. Energy Rev.* **61** 354
[8] Humada A M *et al* 2016 Solar cell parameters extraction based on single and double-diode models: areview *Renew. Sustain. Energy Rev.* **56** 494
[9] Chand S and Kumar J 1995 Current–voltage characteristics and barrier parameters of Pd2Si/p-Si (111) Schottky diodes in a wide temperature range *Semicond. Sci. Technol.* **10** 1680
[10] Ortiz-Conde A, Ma Y, Thomson J, Santos E, Liou J J, García-Sánchez F J, Lei M, Finol J and Layman P 1999 Direct extraction of semiconductor device parameters using lateral optimization method *Solid-State Electron.* **43** 845
[11] Ranuarez J C, García-Sánchez F J and Ortiz-Conde A 1999 Procedure for determining diode parameters at very low forward voltage *Solid-State Electron.* **43** 2129
[12] Ranuarez J C, Ortiz-Conde A and García-Sánchez F J 2000 A new method to extract diode parameters under the presence of parasitic series and shunt resistance *Microelectron. Reliab.* **40** 355
[13] Ortiz-Conde A and García-Sánchez F J 2005 Extraction of non-ideal junction model parameters from the explicit analytic solutions of its *I-V* characteristics *Solid-State Electron.* **49** 465
[14] Mikhelashvili V, Eisenstein G, Garber V, Fainlei S, Bahir G, Ritter D, Orenstein M and Peer A 1999 On the extraction of linear and nonlinear physical parameters in nonideal diodes *J. Appl. Phys.* **85** 6873
[15] Zhang C, Zhang J, Hao Y, Lin Z and Zhu C 2011 A simple and efficient solar cell parameter extraction method from a single current–voltage curve *J. Appl. Phys.* **110** 064504

[16] Hansen C W 2013 Estimation of parameters for single diode models using measured IV curves *39th IEEE Photovoltaic Specialists Conf. (Tampa, FL)* (https://doi.org/10.1109/PVSC.2013.6744135)
[17] Kaminski A, Marchand J J and Laugier A 1999 *I–V* methods to extract junction parameters with special emphasis on low series resistance *Solid-State Electron.* **43** 741
[18] Su H H, Kuo C W and Kitazawa T 2011 A novel approach for modelling diodes into FDTD method *PIERS Proc.* p 20 https://piers.org/piersproceedings/download.php?file=cGllcnMyMDExTWFycmFrZXNofDFBOV8wMTg2LnBkZnwxMDA5MjAwNDMxNDE=
[19] Omar N I C, Hasbullah NF, Rashid NKAM and Abdullah J 2012 Electrical properties of neutron-irradiated silicon and GaAs commercial diodes *IEEE Symp. on Industrial Electronics and Applications (ISIEA)* p 90
[20] Collings P J 1980 Simple measurement of the band gap in silicon and germanium *Am. J. Phys.* **48** 197–9
[21] Orvis W J, Khanaka G H and Yee J H 1987 Development of a GaAs solid state device model for high power applications *Electrical Overstress-Electrostatic Discharge Symp. Proc.* (ESD Association)
[22] Lanyon H P D and Tuft R A 1979 Bandgap narrowing in moderately to heavily doped silicon *IEEE Trans. Electron Devices* **26** 1014
[23] Dhariwal S R and Ojha V N 1985 Some simple observations on the bandgap narrowing in heavily doped silicon *Solid-State Electron.* **28** 845
[24] Fischer C W 1982 Elementary technique to measure the energy band gap and diffusion potential of pn junctions *Am. J. Phys.* **50** 1103
[25] Precker J W and da Silva M A 2002 Experimental estimation of the band gap in silicon and germanium from the temperature-voltage curve of diode thermometers *Am. J. Phys.* **70** 1150
[26] Barkelid M and Zwiller V 2013 Single carbon nanotube photovoltaic device *J. Appl. Phys.* **114** 164320